

Monte Carlo simulations of electromagnetically induced transparency in a square lattice of Rydberg atoms

Shang-Yu Zhai(翟尚宇) and Jin-Hui Wu(吴金辉)

Citation: Chin. Phys. B, 2021, 30 (**7**): 074206. DOI: 10.1088/1674-1056/abd75a
Journal homepage: http://cpb.iphy.ac.cn; http://iopscience.iop.org/cpb

What follows is a list of articles you may be interested in

Sensitivity enhancement of micro-optical gyro with photonic crystal

Liu Yang(杨柳), Shuhua Zhao(赵舒华), Jingtong Geng(耿靖童), Bing Xue(薛冰), and Yonggang Zhang(张勇刚)
Chin. Phys. B, 2021, 30 (**4**): 044208. DOI: 10.1088/1674-1056/abe3f3

Nonlinear spectroscopy of three-photon excitation of cesium Rydberg atoms in vapor cell

Jiabei Fan(樊佳蓓), Yunhui He(何云辉), Yuechun Jiao(焦月春), Liping Hao(郝丽萍), Jianming Zhao(赵建明), and Suotang Jia(贾锁堂)
Chin. Phys. B, 2021, 30 (**3**): 034207. DOI: 10.1088/1674-1056/abca25

Electromagnetically induced transparency and electromagnetically induced absorption in Y-type system

Kalan Mal, Khairul Islam, Suman Mondal, Dipankar Bhattacharyya, Amitava Bandyopadhyay
Chin. Phys. B, 2020, 29 (**5**): 054211. DOI: 10.1088/1674-1056/ab7ea0

Dynamic manipulation of probe pulse and coherent generation of beating signals based on tunneling-induced inference in triangular quantum dot molecules

Nuo Ba(巴诺), Jin-You Fei(费金友), Dong-Fei Li(李东飞), Xin Zhong(钟鑫), Dan Wang(王丹), Lei Wang(王磊), Hai-Hua Wang(王海华), Qian-Qian Bao(鲍倩倩)
Chin. Phys. B, 2020, 29 (**3**): 034204. DOI: 10.1088/1674-1056/ab683d

Electromagnetically induced transparency at optical nanofiber-cesium vapor interface

Rui-Juan Liu(刘瑞娟), Dian-Qiang Su(苏殿强), Zi-Xuan Song(宋子旋), Zhong-Hua Ji(姬中华), Yan-Ting Zhao(赵延霆)
Chin. Phys. B, 2019, 28 (**12**): 124201. DOI: 10.1088/1674-1056/ab4d44

Monte Carlo simulations of electromagnetically induced transparency in a square lattice of Rydberg atoms*

Shang-Yu Zhai(翟尚宇)[1,2] and Jin-Hui Wu(吴金辉)[1,2,†]

[1] *Center for Quantum Sciences, Northeast Normal University, Changchun* 130117, *China*
[2] *School of Physics, Northeast Normal University, Changchun* 130024, *China*

(Received 19 October 2020; revised manuscript received 11 December 2020; accepted manuscript online 30 December 2020)

We study the steady optical response of a square lattice in which all trapped atoms are driven by a probe and a coupling fields into the ladder configuration of electromagnetically induced transparency (EIT). It turns out to be a many-body problem in the presence of van der Waals (vdW) interaction among atoms in the upmost Rydberg state, so Monte Carlo (MC) calculation based on density matrix equations have been done after introducing a sufficiently large cut-off radius. It is found that the absorption and dispersion of EIT spectra depends critically on a few key parameters like lattice dimension, unitary vdW shift, probe Rabi frequency, and coupling detuning. Through modulating these parameters, it is viable to change symmetries of the absorption and dispersion spectra and control on demand depth and position of the transparency window. Our MC calculation is expected to be instructive in understanding many-body quantum coherence effects and in manipulating non-equilibrium quantum phenomena by utilizing vdW interactions of Rydberg atoms.

Keywords: electromagnetically induced transparency, Rydberg atomic lattices, Monte Carlo simulations

PACS: 42.50.Gy, 32.80.Ee, 37.10.Gh **DOI:** 10.1088/1674-1056/abd75a

1. Introduction

Much attention has been paid in theoretical and experimental research on Rydberg atoms considering that they have essential applications, e.g., in the flourishing fields of quantum information and simulation, due to exaggerated properties like long radiative lifetimes, large dipole moments, and strong interatomic interactions.[1–8] In particular, rich many-body behaviors displayed in Rydberg atoms have been found to make a promising prospect for efficiently implementing quantum detection, gates, entanglement, devices, etc. as indispensable elements in future quantum networks.[9–17] Most of these implementations benefit form the so-called dipole blockade or anti-blockade effect, which prohibits or enhances more than one Rydberg excitations in a mesoscopic volume when the energy shift induced by interatomic interactions is prominent or counteracted.[18–21]

Of our special interest, dynamic propagation behaviors of classical or quantized light fields have been well studied in various Rydberg media in the regime of electromagnetically induced transparency (EIT).[22–27] This is a linear optical phenomenon exploiting quantum destructive interference to eliminate (enhance) resonant absorption (dispersion) in coherently dressed multi-level atomic systems, and has been extended to reversible light storage,[28–31] enhanced optical nonlinearities,[32–37] tunable photonic band-gaps,[38,39] etc. Combined with Rydberg atoms, EIT becomes instead a nonlinear optical phenomenon facilitating the efficient generation and manipulation of single-photon sources, switchings, and transistors.[40–43] This is why much work has been done in exploring nontrivial features of the Rydberg-EIT media. In particular, Pritchard *et al.* used EIT technique in a highly excited Rydberg gas and predicted a third-order nonlinearity due to blockade from repulsive interactions.[44] Simons *et al.* studied the effect of band-limited white Gaussian noise on EIT and Autler–Townes (AT) splitting when performing radio-frequency field strength measurements in hot Rydberg atoms.[45] Xu *et al.* proposed an EIT-based scheme to generate stable spatiotemporal solitons in cold Rydberg atoms exhibiting a Bessel lattice potential.[46]

Note however that it is very difficult or impossible to investigate the EIT spectra of randomly distributed Rydberg atoms by solving density matrix equations (DMEs). Great effort has been made to reduce the computation complexity by developing approximation theories for recovering relevant experiments. For instance, a superatom (SA) model developed in the mean field sense is shown to be effective in explaining most spectral features of the Rydberg-EIT media.[47,48] On the other hand, Monte Carlo (MC) simulations based on rate equations (REs) can also reproduce essential Rydberg-EIT features upon the adiabatic elimination of off-diagonal density matrix elements.[8,49] Meanwhile this method is found to be effective in examining non-equilibrium phenomena like antiferromagnetic phases, bistable phases, and topological superfluids in two-dimensional lattices of periodically distributed Rydberg atoms.[50–55]

Here we investigate the steady EIT spectra of cold Ryd-

*Project supported by the National Natural Science Foundation of China (Grant No. 12074061).
†Corresponding author. E-mail: jhwu@nenu.edu.cn
© 2021 Chinese Physical Society and IOP Publishing Ltd

berg atoms arranged into a square lattice via MC simulations based on both DMEs and REs. A direct comparison shows that DMEs are more accurate than REs especially when the Rydberg lattice has a large dimension and thus complicated van der Waals (vdW) interactions. We find in particular that the absorption and dispersion of EIT spectra become more and more asymmetric until reaching the saturation regime as the lattice dimension increases. More importantly, the transparency window as a main EIT sign typically suffer from a notable reduction in depth due to dephasings arising from the inhomogeneous vdW interactions. The center of this transparency window is determined however by the average value of vdW induced level shifts. These nontrivial features are evident only when the probe field is not too weak and may also be controlled by modulating the coupling field detuning to counteract the average vdW shift.

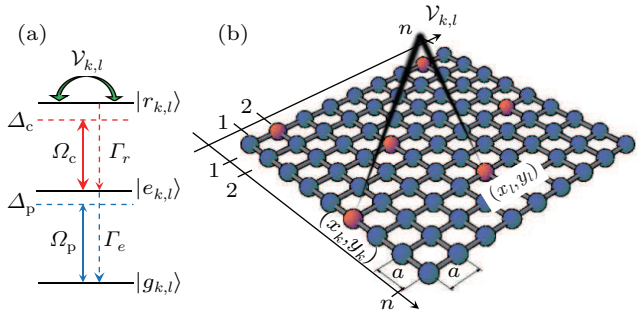


Fig. 1. (a) A three-level ladder atomic system with ground state $|g\rangle$, intermediate state $|e\rangle$, and Rydberg state $|r\rangle$ driven by a probe field Ω_p and a coupling field Ω_c (see text for more details). (b) A $n\times n$ atomic array of period a in which each atom is driven into the three-level ladder configuration and interacts with another atom via the vdW potential $\mathcal{V}_{kl}$ if both are in state $|r\rangle$ (see text for more details).

2. Model and equations

We consider a ladder configuration [see Fig. 1(a)] with ground state $|g\rangle$, intermediate state $|e\rangle$, and Rydberg state $|r\rangle$ as driven by a strong coupling field of Rabi frequency (detuning) Ω_c (Δ_c) and a weak probe field of Rabi frequency (detuning) Ω_p (Δ_p). Then a square array of $N=n\times n$ such ladder-type atoms trapped, e.g., in 2D optical lattices of period a [see Fig. 1(b)] can be described by the following interaction Hamiltonian:

$$\begin{aligned}\mathcal{H}_I &= \mathcal{H}_\Delta+\mathcal{H}_\Omega,\\ \mathcal{H}_\Delta &= \sum_{k=1}^{N}-\Delta_p|e_k\rangle\langle e_k|-(\Delta_c+\mathcal{V}_k)|r_k\rangle\langle r_k|,\\ \mathcal{H}_\Omega &= \sum_{k=1}^{N}\left(\Omega_p|e_k\rangle\langle g_k|+\Omega_c|r_k\rangle\langle e_k|+\text{h.c.}\right),\end{aligned}\tag{1}$$

where $\mathcal{V}_k=\sum_{l\neq k}\mathcal{V}_{kl}=C_6\sum_{l\neq k}|r_l\rangle\langle r_l|/|r_k-r_l|^6$ denotes the vdW induced shift for atom k contributed by all other atoms, and C_6 is the vdW coefficient. For convenience in the following discussion, we further choose to label atom k by its coordinate $r_k=(x_k,y_k)a$ with integers $x_k\in\{1,2,\ldots,n\}$ and $y_k\in\{1,2,\ldots,n\}$ and define $\mathcal{V}_0=C_6/a^6$ as the unitary vdW induced shift.

Atom k in states $|r_k\rangle$ and $|e_k\rangle$ will decay via spontaneous emission to states $|e_k\rangle$ and $|g_k\rangle$ at rates Γ_r and Γ_e, respectively. Considering a Rydberg state is typically long lived, we may set $\Gamma_r\to 0$ and obtain from H_I the following density matrix equations (DMEs):

$$\begin{aligned}\partial_t\rho_{gg}^{(k,l)} &= (\mathrm{i}\Omega_p\rho_{ge}^{(k,l)}+\text{h.c.})+\Gamma_e\rho_{ee}^{(k,l)},\\ \partial_t\rho_{ee}^{(k,l)} &= (\mathrm{i}\Omega_c\rho_{er}^{(k,l)}-\mathrm{i}\Omega_p\rho_{ge}^{(k,l)}+\text{h.c.})-\Gamma_e\rho_{ee}^{(k,l)},\\ \partial_t\rho_{ge}^{(k,l)} &= -\gamma_{ge}\rho_{ge}^{(k,l)}-\mathrm{i}\Omega_p(\rho_{ee}^{(k,l)}-\rho_{gg}^{(k,l)})+\mathrm{i}\Omega_c\rho_{gr}^{(k,l)},\\ \partial_t\rho_{gr}^{(k,l)} &= -\gamma_{gr}^{(k)}\rho_{gr}^{(k,l)}-\mathrm{i}\Omega_p\rho_{er}^{(k,l)}+\mathrm{i}\Omega_c\rho_{ge}^{(k,l)},\\ \partial_t\rho_{er}^{(k,l)} &= -\gamma_{er}^{(k)}\rho_{er}^{(k,l)}-\mathrm{i}\Omega_c(\rho_{rr}^{(k,l)}-\rho_{ee}^{(k,l)})-\mathrm{i}\Omega_p\rho_{gr}^{(k,l)},\end{aligned}\tag{2}$$

for atom k in the l realization. We have set in Eq. (2) $\rho_{\mu\nu}^{(k,l)*}=\rho_{\nu\mu}^{(k,l)}$ and $\rho_{gg}^{(k,l)}+\rho_{ee}^{(k,l)}+\rho_{rr}^{(k,l)}=1$ so that $\gamma_{ge}=\Gamma_e/2+\mathrm{i}\Delta_p$, $\gamma_{gr}^{(k)}=\mathrm{i}(\Delta_p+\Delta_c+\mathcal{V}_k)$, and $\gamma_{er}^{(k)}=\Gamma_e/2+\mathrm{i}(\Delta_c+\mathcal{V}_k)$. This set of many-body DMEs can be reduced into those for a two-level Rydberg model in the case of $\Omega_c\ll\Omega_p$,[49] which is impracticable however in the case of $\Omega_c\gg\Omega_p$ of our present interest.

Assuming sufficiently strong decoherence on the probe transition ($\Gamma_e\gg\Omega_p$), however, it is viable to adiabatically eliminate the off-diagonal matrix elements in Eq. (2) by setting $\partial_t\rho_{\mu\nu}=0$ ($\mu\neq\nu$) to attain the following set of reduced rate equations (REs):

$$\frac{\partial}{\partial t}\begin{pmatrix}\rho_{gg}^{(k,l)}\\ \rho_{ee}^{(k,l)}\\ \rho_{rr}^{(k,l)}\end{pmatrix}=\begin{pmatrix}R_{gg}^{(k,l)} & R_{ge}^{(k,l)} & R_{gr}^{(k,l)}\\ R_{eg}^{(k,l)} & R_{ee}^{(k,l)} & R_{er}^{(k,l)}\\ R_{rg}^{(k,l)} & R_{re}^{(k,l)} & R_{rr}^{(k,l)}\end{pmatrix}\begin{pmatrix}\rho_{gg}^{(k,l)}\\ \rho_{ee}^{(k,l)}\\ \rho_{rr}^{(k,l)}\end{pmatrix},\tag{3}$$

which are much easier to solve than Eq. (2) in regard of a many-body quantum problem. From the steady solutions of Eq. (3) in the case of $\Delta_c=0$, it is straightforward to attain the off-diagonal matrix element

$$\rho_{ge}^{(k,l)}=\frac{a_1\left(\rho_{gg}^{(k,l)}-\rho_{ee}^{(k,l)}\right)+a_2\left(\rho_{ee}^{(k,l)}-\rho_{rr}^{(k,l)}\right)}{b_1\mathcal{V}_k^2+b_2\mathcal{V}_k+b_3},\tag{4}$$

with

$$\begin{aligned}a_1 &= \Omega_p\left[-4\mathrm{i}\mathcal{V}_k^2-(4\mathrm{i}\Delta_p+2\Gamma_e)\Omega_p\mathcal{V}_k+\mathrm{i}\Omega_p^2-2\Delta_p\Gamma_e\right],\\ a_2 &= \mathrm{i}\Omega_p\Omega_c^2,\\ b_1 &= -4\Gamma_e-8\mathrm{i}\Delta_p,\\ b_2 &= -8\mathrm{i}\Delta_p^2-8\Delta_p\Gamma_e+2\mathrm{i}\Gamma_e^2+2\mathrm{i}\Omega_c^2,\\ b_3 &= 2\mathrm{i}\Delta_p(\Gamma_e^2+\Omega_p^2)+\Gamma_e(\Omega_p^2-\Omega_c^2-4\Delta_p^2),\end{aligned}$$

which determines the absorption and dispersion properties on the probe transition and is contributed by both population differences $\rho_{gg}^{(k,l)}-\rho_{ee}^{(k,l)}$ and $\rho_{ee}^{(k,l)}-\rho_{rr}^{(k,l)}$. Equation (4) can be largely simplified in the case of $\mathcal{V}_k\to 0$, e.g., in sparse enough atomic lattices.

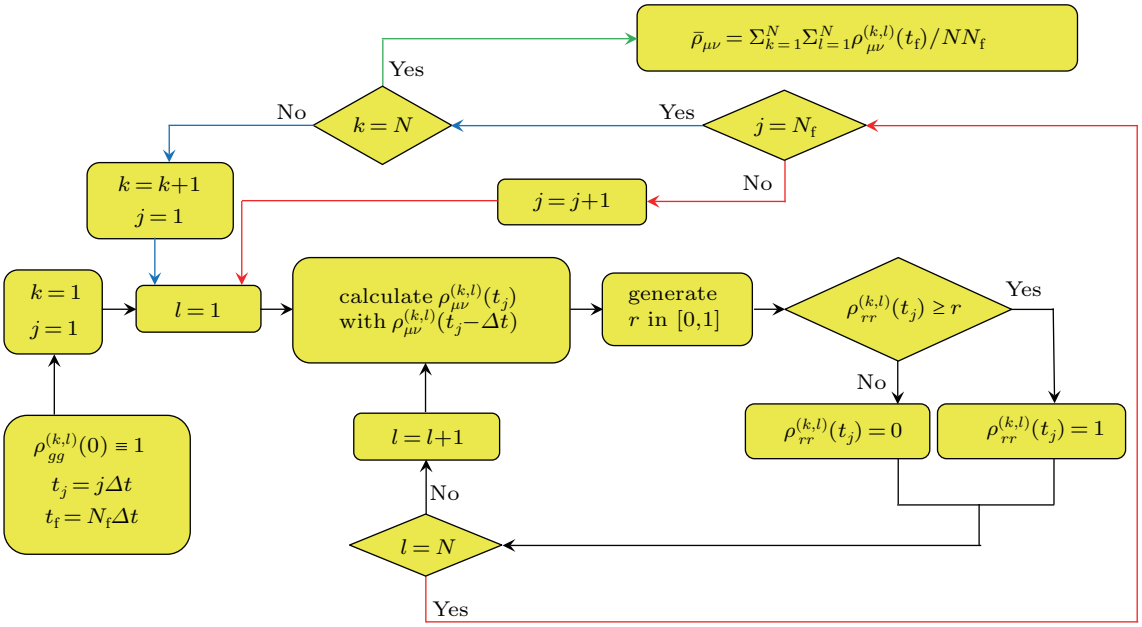


Fig. 2. Flow chart for a single realization of the Monte Carlo method used to calculate the averaged values of density matrix elements $\bar{\rho}_{\mu\nu}$ in the steady state at time $t_{\rm f}=20$ μs.

When solving Eq. (2) or Eq. (3), we should resort to the MC method as described in Fig. 2. In each realization, at the starting time $t_0=0$, all atoms in the 2D lattices are first assumed to be in the ground state with $\rho_{gg}^{(k,l)}(t_0)=1$. Then, we calculate matrix elements $\rho_{\mu\nu}^{(k,l)}(t_1)$ at time t_1 with their counterparts at time t_0 for all atoms one by one in the order of $k\in\{(1,1),\ldots,(1,n);(2,1),\ldots,(2,n);\ldots;(n,1),\ldots,(n,n)\}$, and reset $\rho_{rr}^{(k,l)}(t_1)=1$ ($\rho_{rr}^{(k,l)}(t_1)=0$) if $\rho_{rr}^{(k,l)}(t_1)>r_k$ ($\rho_{rr}^{(k,l)}(t_1)<r_k$), $r_k\in\{0,1\}$ being a randomly generated number. In the same sense, we can calculate matrix elements $\rho_{\mu\nu}^{(k,l)}(t_j)$ at time t_j with their counterparts at time t_{j-1} and determine $\rho_{rr}^{(k,l)}(t_j)=1$ or $\rho_{rr}^{(k,l)}(t_j)=0$ until reaching the steady state at a large enough final time $t_{\rm f}$. The above MC processes will be repeated, e.g., $N_{\rm f}=100$ times so that the random fluctuations of our numerical results can be smoothed by taking the average of all $N_{\rm f}$ realizations. That is, the final average result is given by $\bar{\rho}_{\mu\nu}=\sum_{k=1}^{N}\sum_{l=1}^{N_{\rm f}}\rho_{\mu\nu}^{(k,l)}/NN_{\rm f}$.

To be more concrete, we now take the three levels in our ladder model as $|g\rangle\equiv|5S_{1/2},F=2,m_F=2\rangle$, $|e\rangle\equiv|5P_{1/2},F=1,m_F=1\rangle$, and $|r\rangle\equiv|60S_{1/2},m_J=1\rangle$ of cold ^{87}Rb atoms, respectively.[47] In this case, we have $\Gamma_e/2\pi\simeq 6.0$ MHz, $\Gamma_r/2\pi\simeq 2.0$ kHz, and $C_6/2\pi=140$ GHz·μm^6. In the following, we further set $\Omega_{\rm p}=0.3$ MHz and $\Omega_{\rm c}=3.0$ MHz, $\Delta_{\rm p}=0$, and $\mathcal{V}_0=64.3$ MHz for $a=3.6$ μm (a); $\mathcal{V}_0=130.4$ MHz for $a=3.2$ μm (b); $\mathcal{V}_0=290.5$ MHz for $a=2.8$ μm (c) to plot in Fig. 3 the average Rydberg population $\bar{\rho}_{rr}$ against a cut-off radius $R_{\rm c}$. Note that it is viable to create a 2D trap lattice (array) of period $a\simeq 3.0$ μm using a spatial light modulator to manipulate a dipole-trap beam, into which cold single ^{87}Rb atoms can be loaded from a magneto-optical trap.[56] It is clear that $R_{\rm c}=4a$ is enough to guarantee an accurate calculation of $\bar{\rho}_{rr}$, indicating atoms outside the circle of radius $R_{\rm c}=4a$ has negligible influences on atom k at the center. Introduction of $R_{\rm c}$ is beneficial to largely reduce the heavy computation tasks in solving a many-body quantum system. Based on simulations in Fig. 3, it is also found that our square atomic lattice will enter the steady state for $t_{\rm f}\simeq 20$ μs. In other methods based on mean-field approximations,[42] the atomic sample is usually divided into many independent volumes of blockade radius $R_{\rm b}=(C_6\Gamma_e/2\Omega_{\rm c}^2)^{1/6}$, and vdW interactions are assumed to occur only inside each blockade volume. For our used parameters, it is easy to find that $R_{\rm b}=6.0$ μm is smaller than $R_{\rm c}=4a$ so that accurate results cannot be attained if we simply set $R_{\rm c}=R_{\rm b}$.

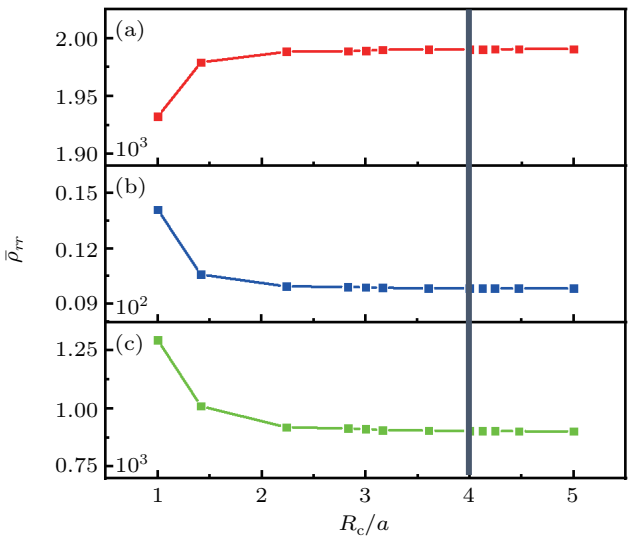


Fig. 3. Averaged Rydberg population $\bar{\rho}_{rr}$ against cut-off radius $R_{\rm c}$ with $\mathcal{V}_0=64.3$ MHz (a), $\mathcal{V}_0=130.4$ MHz (b), and $\mathcal{V}_0=290.5$ MHz (c), respectively. Other parameters used in calculations are given in the main text.

3. Results and discussion

Based on the MC method, we now examine in Fig. 4 the dependence of absorption $\mathrm{Im}(\bar{\rho}_{ge})$ and dispersion $\mathrm{Re}(\bar{\rho}_{ge})$ properties on probe detuning Δ_p for a few square lattices of different dimensions. Typical absorption and dispersion spectra in ordinary EIT media, i.e., a transparent window of mirror symmetry and a normal dispersion of rotation symmetry centered at $\Delta_\mathrm{p} = 0$, are observed for $n = 1$ because vdW interactions won't occur for a single atom. As n increases, both absorption and dispersion spectra first suddenly deviate from their original symmetries because vdW interactions start to take place, and then slowly approach a saturation situation. To be more concrete, as lattice dimension n increases, a higher proportion of atoms will become far away from boundaries to interact via the vdW shift $\mathcal{V}_k$ with the same number of neighboring atoms in the cut-off radius. Meanwhile, atoms at or close to boundaries will take a lower proportion and interact with (less) different numbers of neighboring atoms. In this case, a saturation regime can be reached as lattice dimension n is large enough so that the number of atoms at or close to boundaries can be neglected as compared to that of others. This is evident by noting that the transparent window's center is finally stabilized at $\Delta_\mathrm{p}/2\pi \simeq -1.63$ MHz for $n \lesssim 50$. That means, each atom suffers from an average vdW shift $\bar{\mathcal{V}}/2\pi \simeq 1.63$ MHz as contributed by its neighboring atoms because $\bar{\mathcal{V}}$ works indeed as an effective detuning of the coupling field. It is worth noting that the average vdW shift is determined by the vdW coefficient, the average Rydberg population, and the atomic number in the cut-off radius. A depth reduction of the transparency window is also evident for $n = 10$ and $n = 50$ due to additional dephasings arising from the inhomogeneity of vdW shift $\mathcal{V}_k$. We further note that MC calculations based on DMEs are somewhat different from those based on REs, indicating the adiabatic elimination of off-diagonal matrix elements $\rho_{\mu\nu}$ will result in more or less coherent information loss, especially for a large atomic lattice.

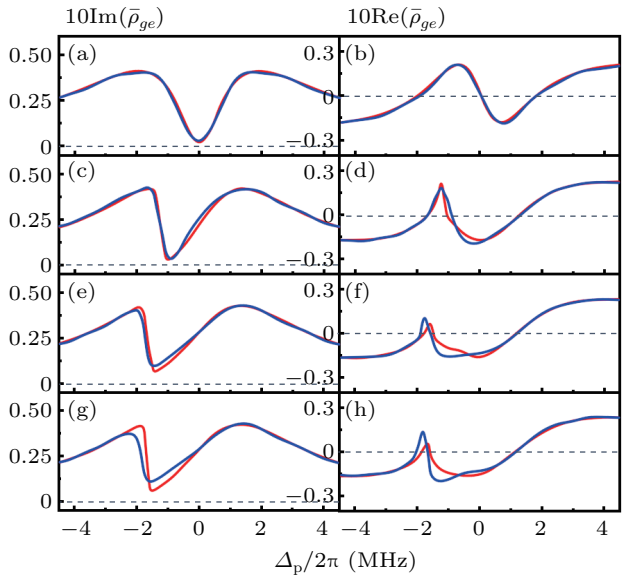


Fig. 4. Absorption $\mathrm{Im}(\bar{\rho}_{ge})$ (left) and dispersion $\mathrm{Re}(\bar{\rho}_{ge})$ (right) properties against probe detuning Δ_p attained via Monte Carlo calculations based on DMEs (red-solid) and REs (blue-dashed) with $n = 1$ (a), (b), $n = 2$ (c), (d), $n = 10$ (e), (f), and $n = 50$ (g), (h), respectively. Other parameters are the same as in Fig. 3 except $\mathcal{V}_0 = 64.3$ MHz.

It is not difficult to imagine that the spectra of absorption and dispersion will finally recover those for two-level absorbing atoms as vdW interactions are sufficiently strong. In this case, a large enough average vdW shift $\bar{\mathcal{V}}$ works as an infinite effective detuning of the coupling field so that it is decoupled from the upper transition, yielding thus a two-level system involving only the lower transition. This is confirmed in Fig. 5, where a square lattice of $n = 50$ is considered for three values of $\mathcal{V}_0$. We find in particular that the transparency window becomes shallower and the dispersion slope becomes smoother as the lattice period a is reduced to attain a larger $\mathcal{V}_0$. It is also worth noting that the centers of absorption and dispersion curves move left together so that their right parts become more important and thus look more like those for two-level absorbing atoms. This means that the lattice period a or the atomic density $1/a^2$ should be carefully chosen to manipulate the blockade effect for attaining a desired optical response in a square lattice of Rydberg atoms. To be more concrete, a smaller lattice period will result in a higher atomic density and thus a stronger blockade effect because larger average vdW shifts can be attained to yield weaker atom-field couplings when more atoms are found in the cut-off radius.

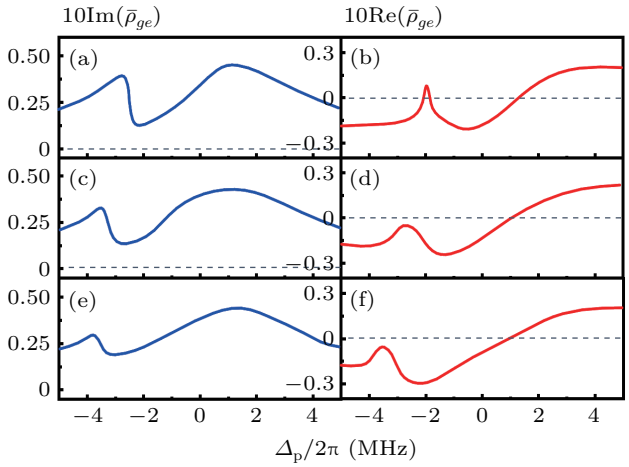


Fig. 5. Absorption $\mathrm{Im}(\bar{\rho}_{ge})$ (left) and dispersion $\mathrm{Re}(\bar{\rho}_{ge})$ (right) properties against probe detuning Δ_p for a square lattice of $n = 50$ with $\mathcal{V}_0 = 130.4$ MHz (a), (b), $\mathcal{V}_0 = 290.5$ MHz (c), (d), and $\mathcal{V}_0 = 360.0$ MHz (e), (f), respectively. Other parameters are the same as in Fig. 3.

We then check in Fig. 6 how the spectra of absorption and dispersion depend on the Rabi frequency of probe field for a square lattice of $n = 50$. It is clear that both $\mathrm{Im}(\bar{\rho}_{ge})$ and $\mathrm{Re}(\bar{\rho}_{ge})$ exhibit a nonlinear dependence on Ω_p, manifested as a notable change of the transparency window both in depth and in position. To be more concrete, the spectra of absorption and dispersion are found to recover those for a single atom as Ω_p

decreases from 0.3 MHz to 0.03 MHz, but become more asymmetric with a shallower transparency window as $\Omega_{\rm p}$ increases from 0.3 MHz to 0.9 MHz. This is a strong evidence of the so-called cooperative nonlinearity[8,39] due to long-range vdW interactions among Rydberg atoms. Different from atomic samples of random spatial distributions, a much larger deviation of the transparency window from its original center is found for our atomic lattice of a periodic spatial distribution.

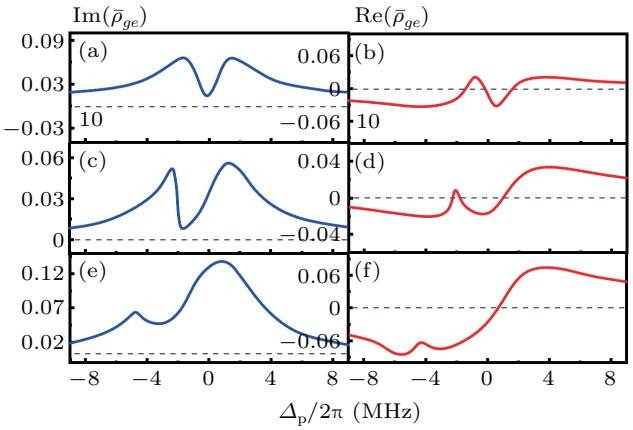


Fig. 6. Absorption Im($\bar{\rho}_{ge}$) (left) and dispersion Re($\bar{\rho}_{ge}$) (right) properties against probe detuning $\Delta_{\rm p}$ for a square lattice of $n = 50$ with $\Omega_{\rm p} = 0.03$ MHz (a), (b), $\Omega_{\rm p} = 0.3$ MHz (c), (d), and $\Omega_{\rm p} = 0.9$ MHz (e), (f), respectively. Other parameters are the same as in Fig. 3 except $\mathcal{V}_0 = 64.3$ MHz.

Finally, we show how to control the absorption and dispersion of the EIT spectra by modulating the coupling field detuning to compensate more or less the vdW shift for a square lattice of $n = 50$. As can be seen from Fig. 7, the absorption and dispersion curves disturbed by the coupling field detuning do not exhibit mirror and rotation symmetries like those for a single atom even if the transparency window is centered again at $\Delta_{\rm p} \simeq 0$ for $\Delta_{\rm c}/2\pi \simeq -2.0$ MHz. In this case, the average vdW shift is estimated to be $\bar{\mathcal{V}}/2\pi \simeq 2.0$ MHz because a transparency window centered at $\Delta_p = 0$ requires a vanishing effective detuning $\Delta_{\rm c} + \bar{\mathcal{V}} = 0$. This average vdW shift $\bar{\mathcal{V}}$ is slightly different from that estimated in Fig. 4 because it depends on the Rydberg population $\bar{\rho}_{rr}$ and thus the coupling detuning $\Delta_{\rm c}$. We further find that the transparency window moves left (right) for a larger (smaller) $\Delta_{\rm c}$ to result in more asymmetric absorption and dispersion curves, but the transparency window's depth does not change too much as $\Delta_{\rm c}$ is modulated to control the transparency window's position. Such a control of the transparency window is clearly different from those shown in Figs. 4–6 by modulating other parameters. The underlying physics is that the Rydberg population ρ_{rr} depends on but is not very sensitive to the coupling field detuning in the case of a relatively weak probe field ($\Omega_{\rm p} = 0.3$ MHz vs. $\Gamma_e = 6.0$ MHz), so that dephasings arising from the inhomogeneity of vdW shift $\mathcal{V}_k$ do not change evidently as $\Delta_{\rm c}$ changes.

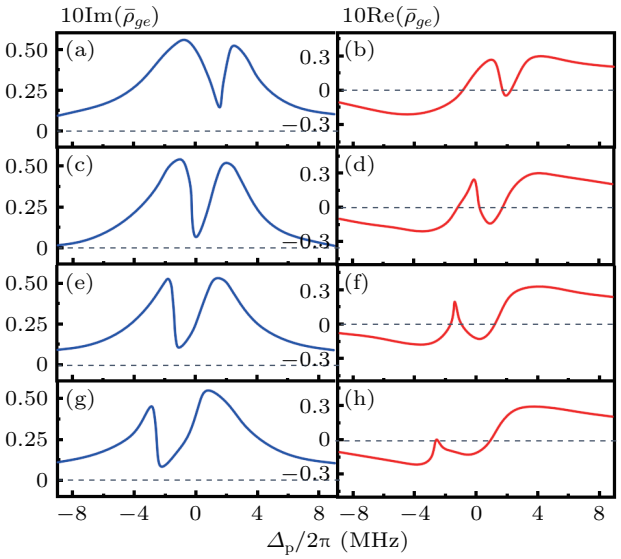


Fig. 7. Absorption Im($\bar{\rho}_{ge}$) (left) and dispersion Re($\bar{\rho}_{ge}$) (right) properties against probe detuning $\Delta_{\rm p}$ for a square lattice of $n = 50$ with $\Delta_{\rm c} = -3.0$ MHz (a), (b); $\Delta_{\rm c} = -2.0$ MHz (c), (d); $\Delta_{\rm c} = -0.5$ MHz (e), (f); $\Delta_{\rm c} = 0.5$ MHz (g), (h). Other parameters are the same as in Fig. 3 except $\mathcal{V}_0 = 64.3$ MHz.

4. Conclusion

In summary, we have studied a square lattice of Rydberg atoms in the ladder configuration by examining its EIT spectra of absorption and dispersion in the presence of vdW interactions. Monte Carlo calculations based on density matrix equations show that the EIT spectra becomes more and more asymmetric, until the transparency window finally centered at a position determined by the average vdW shift $\bar{\mathcal{V}}$, as the lattice dimension n increases. The transparency window is found in particular to suffer from a notable reduction in depth due to the additional dephasings arising from the inhomogeneity of vdW interactions. These features are evident only when the probe Rabi frequency $\Omega_{\rm p}$ is not too small and may turn out to be those for two-level absorbing atoms as the unitary vdW shift $\mathcal{V}_0$ is large enough. Moreover, it is convenient to control these features (e.g., roughly recover the symmetric EIT spectra) by modulating the coupling detuning $\Delta_{\rm c}$ to counteract the average vdW shift $\bar{\mathcal{V}}$. Our Monte Carlo calculations are more accurate than calculations based on mean-field approximations[47] and may be extended to study other properties like non-equilibrium physics[50] in finite lattices of Rydberg atoms.

References

[1] Mohapatra A K, Jackson T R and Adams C S 2007 *Phys. Rev. Lett.* **98** 113003
[2] Mauger S, Millen J and Jones M P A 2007 *J. Phys. B: At. Mol. Opt. Phys.* **40** F319
[3] Mohapatra A K, Bason M G, Butscher B, Weatherill K J and Adams C S 2008 *Nat. Phys.* **4** 890
[4] Zhang L J, Bao S X, Zhang H and Raithel G 2017 arXiv: 1702.04842 [physics.atom-ph]
[5] Zhao J, Zhu X, Zhang L, Feng Z, Li C and Jia S 2009 *Opt. Express* **17** 15821

[6] Kubler H, Shaffer J P, Baluktsian T, Low R and Pfau T 2010 *Nat. Photon.* **4** 112

[7] Tauschinsky A, Thijssen R M T, Whitlock S, van Linden van den Heuvell H B and Spreeuw R J C 2010 *Phys. Rev. A* **81** 063411

[8] Ates C, Sevincli S and Pohl T 2011 *Phys. Rev. A* **83** 041802

[9] Sedlacek J A, Schwettmann A, Kubler H and Shaffer J P 2013 *Phys. Rev. Lett.* **111** 063001

[10] Brion E, Pedersen L H and Molmer K 2007 *J. Phys. B* **40** S159

[11] Muller M, Lesanovsky I, Weimer H, Buchler H P and Zoller P 2009 *Phys. Rev. Lett.* **102** 170502

[12] Moller D, Madsen L B and Molmer K 2008 *Phys. Rev. Lett.* **100** 170504

[13] Rao D D B and Molmer K 2013 *Phys. Rev. Lett.* **111** 033606

[14] Wuster S, Mobius S, Genkin M, Eisfeld A and Rost J M 2013 *Phys. Rev. A* **88** 063644

[15] Baur S, Tiarks D, Rempe G and Durr S 2014 *Phys. Rev. Lett.* **112** 073901

[16] Tiarks D, Baur S, Schneider K, Durr S and Rempe G 2014 arXiv: 1404.3061 [quant-ph]

[17] Zhang Q R, Wang B B, Zhang M L and Yan D 2018 *Acta Phys. Sin.* **67** 034202 (in Chinese)

[18] Peyronel T, Firstenberg O, Liang Q Y, Hofferberth S, Gorshkov A V, Pohl T, Lukin M D and Vuletic V 2012 *Nature* **488** 57

[19] Huang J F, Liao J Q and Sun C P 2013 *Phys. Rev. A* **87** 023822

[20] Muller M M, Kolle A, Low R, Pfau T, Calarco T and Montangero S 2013 *Phys. Rev. A* **87** 053412

[21] Tong D, Farooqi S M, Stanojevic J, Krishnan S, Zhang Y P, Cote R, Eyler E E and Gould P L 2004 *Phys. Rev. Lett.* **93** 063001

[22] Harris S E 1997 *Phys. Today* **50** 36

[23] Fleischhauer M, Imamoglu A and Marangos J P 2005 *Rev. Mod. Phys.* **77** 633

[24] Weatherill K J, Pritchard J D, Abel R P, Bason M G, Mohapatra A K and Adams C S 2008 *J. Phys. B: At. Mol. Opt. Phys.* **41** 201002

[25] Pritchard J D, Maxwell D, Gauguet A, Weatherill K J, Jones M P A and Adams C S 2010 *Phys. Rev. Lett.* **105** 193603

[26] Yang Z W, Jiao Y C, Han X X, Zhao J M and Jia S T 2016 *Acta Phys. Sin.* **65** 103201 (in Chinese)

[27] Yang Z W, Jiao Y C, Han X X, Zhao J M and Jia S T 2017 *Acta Phys. Sin.* **66** 093202 (in Chinese)

[28] Liu C, Dutton Z, Behroozi C H and Hau L 2001 *Nature* **409** 490

[29] Chaneliere T, Matsukevich D N, Jenkins S D, Lan S Y, Kennedy T A B and Kuzmich A 2005 *Nature* **438** 833

[30] Zhang Y, Zhang Y, Zhang X H, Yu M, Cui C L and Wu J H 2012 *Phys. Lett. A* **376** 656

[31] Appel J, Figueroa E, Korystov D, Lobino M and Lvovsky A I 2008 *Phys. Rev. Lett.* **100** 093602

[32] Harris S E and Hau L V 1999 *Phys. Rev. Lett.* **82** 4611

[33] Lukin M D and Imamoglu A 2001 *Nature* **413** 273

[34] Kang H and Zhu Y 2003 *Phys. Rev. Lett.* **91** 093601

[35] Li S J, Yang X D, Cao X M, Zhang C H, Xie C D and Wang H 2008 *Phys. Rev. Lett.* **101** 073602

[36] Ba N, Wan R G, Jiang B N, Wang H, Wang D W, Zhang Y and Wu J H 2010 *Opt. Commun.* **283** 1017

[37] Yan D, Wang B B, Bai W J, Liu B, Du X G and Ren C N 2019 *Acta Phys. Sin.* **68** 084203 (in Chinese)

[38] Artoni M and LaRocca G C 2006 *Phys. Rev. Lett.* **96** 073905

[39] Zhang Y, Xue Y, Wang G, Cui C L, Wang R G and Wu J H 2011 *Opt. Express* **19** 2111

[40] Miller J L 2012 *Phys. Today* **65** 14

[41] Baur S, Tiarks D, Rempe G and Durr S 2014 *Phys. Rev. Lett.* **112** 073901

[42] Gorniaczyk H, Tresp C, Bienias P, ParisMandoki A and Hofferberth S 2016 *Nat. Commun.* **7** 12480

[43] Zhao J D, Zhang H, Yang W G, Zhao J H, Jing M Y and Zhang L J 2021 *Acta Phys. Sin.* **70** 103201 (in Chinese)

[44] Pritchard J D, Gauguet A and Weatherill K J 2011 *J. Phys. B* **44** 184019

[45] Simons M T, Kautz M D, Holloway C L, Anderson D A, Raithel G, Stack D, St John M C and Su W 2018 *J. Appl. Phys.* **123** 203105

[46] Xu S L, Zhou Q, Zhao D, Belic M R and Zhao Y 2020 *Appl. Math. Lett.* **106** 106230

[47] Petrosyan D, Otterbach J and Fleischhauer M 2011 *Phys. Rev. Lett.* **107** 213601

[48] Liu Y M, Yan D, Tian X D, Cui C L and Wu J H 2014 *Phys. Rev. A* **89** 033839

[49] Ates C, Pohl T, Pattard T and Rost J M 2007 *Phys. Rev. A* **76** 013413

[50] Hoening M, Abdussalam W, Fleischhauer M and Pohl T 2014 *Phys. Rev. A* **90** 021603

[51] Sibali N, Wade C G, Adams C S, Weatherill K J and Pohl T 2016 *Phys. Rev. A* **94** 011401

[52] Gorshkov A V, Manmana S R, Chen G, Ye J, Demler E, Lukin M D and Rey A M 2011 *Phys. Rev. Lett.* **107** 115301

[53] Moses S A, Covey J P, Miecnikowski M T, Yan B, Gadway B, Ye J and Jin D S 2015 *Science* **6** 659

[54] Zhang Z J, Peng Y D, Li C, Jia Z M, Li D H and Zeng Q T 2019 *J. Opt. Soc. Am. B* **36** 2216

[55] Cooper N R and Shlyapnikov G V 2009 *Phys. Rev. Lett.* **103** 155302

[56] Labuhn H, Barredo D, Ravets S, Léséleuc S, Macrì T, Lahaye T and Browaeys A 2016 *Nature* **534** 667